

ARTICLE

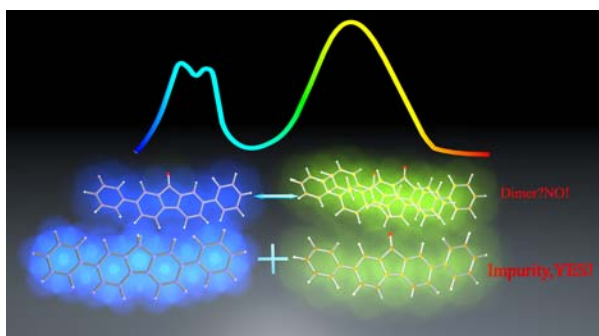
Aggregation-Induced Emission with Large Redshift in 2,7-Diphenylfluorenone: Reality or Artifact?[†]

Xinmao Li, Jianxin Guan, Chuanqing Hao, Zhihao Yu, Junrong Zheng*

College of Chemistry and Molecular Engineering, Beijing National Laboratory for Molecular Sciences, Peking University, Beijing 100871, China

(Dated: Received on October 16, 2021; Accepted on November 8, 2021)

The luminescence property of 2,7-diphenylfluorenone (DPFO) was previously reported to be very unusual with a large aggregation-induced effect associated with a fluorescence redshift of 150 nm. The phenomenon is reexamined in this work. It is found that the abnormal observations are caused by the presence of a trace amount of impurity



2,7-diphenylfluorene (DPF) in the as-synthesized DPFO. The pure DPFO molecule does have an intense fluorescence (FL) in solid (528 nm), about 4–5 times larger than in its dilute dichloromethane solutions (542 nm), but with a blueshifted rather than redshifted FL wavelength in solid. The enormous FL enhancement and redshifted FL wavelength of the as-synthesized DPFO solid are due to the presence of impurity DPF. The FL of DPF is much stronger than that of DPFO in dilute solutions and it also has shorter FL wavelengths. In a dilute solution of DPFO with a trace amount of DPF (~1%), the dominant FL peaks are from DPF. Because the electronic absorption peaks of DPF overlaps with DPFO, the electronic energy of DPF can transfer to DPFO. The energy transfer is faster with the increase of concentration because DPF and surrounding DPFO molecules become closer, which quenches the FL of DPF (356 and 372 nm) and enhances the FL of DPFO (542 nm in solution and 528 nm in solid). Therefore, at high concentrations or in solids, only peak at about 542 or 528 nm shows up, and peaks at 356 and 372 nm disappear.

Key words: Aggregation-induced emission, Fluorescence, Impurity, Fluorenone

I. INTRODUCTION

The fluorescence quantum yields and wavelengths of many luminescent molecules are closely correlated to their molecular states which may affect their electronic transition dipole moments and/or nonradiative decay

dynamics. Many molecules fluoresce strongly in dilute solutions but dim in concentrated solutions or in solids, a phenomenon known as aggregation-induced quenching (ACQ) [1]. In contrast, there is a group of molecules with weak fluorescence or even no luminescence in dilute solutions, but with very high emission quantum yields in aggregated states. These molecules are aggregation-induced emission (AIE) molecules [2]. The AIE phenomenon was reported as early as in 1896 [3]. At the beginning of the 21st century, AIE begins to attract extensive research attention due to their abnormal optical properties and potential applications in solid state

[†]Part of Special Issue “John Z.H. Zhang Festschrift for celebrating his 60th birthday”.

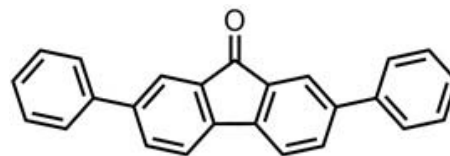
*Author to whom correspondence should be addressed. E-mail: junrong@pku.edu.cn

luminescence, photoelectronic devices, biosensing, and many other fields [4, 5].

Although AIE has a long history, its mechanism has been controversial for many years. Recently, research combining ultrafast ultraviolet/infrared spectroscopy measurements and theoretical calculations rationalizes the mechanism for traditional AIE molecules, like tetraphenyl ethylene (TPE) [6]. It is revealed that the low emission quantum yield in dilute solutions results from the rapid nonradiative decay of the electronic excited state by crossing conical intersections (CI), whereas in solids the energy barriers are too high for the excited molecule to cross CI, and the bulky side groups well separate molecules so energy/electronic transfers are slow inside the solids. The combination of the two factors causes the abnormal AIE phenomenon.

In addition to traditional AIE molecules mentioned above, some other molecular systems may have quantum efficiencies significantly different in solutions from those in the aggregate states. For example, H-aggregation [7] or J-aggregation [8] can significantly change the luminescence behavior of molecules. Besides, the formation of dimer or excimer can also significantly change the luminescence behavior of molecules [9]. In principle, the correlation between fluorescence quantum yield and molecular states can be well explained with spontaneous emission and nonradiative decays caused by the energy transfer dephasing mechanism and crossing conical intersections [10].

In 2014, a very unusual aggregation-induced effect was reported [11] in a series of 2,7-substituted fluorenone derivatives. In dilute solutions, the fluorescence wavelengths of these molecules are located in the ultraviolet region, and the quantum yield is only about 1%. In solids, their fluorescence peaks redshift for about 150 nm, and the quantum yields increase significantly, reaching 60%. The observations are very different from two types of well-known AIE: (i) the typical AIE molecules with bulky side groups like TPE fluoresce strongly in solids but with a slightly blueshifted wavelength due to the less conjugated molecular structure, compared to its dilute solution [2]; (ii) molecules with lone electron pairs like amine molecules do not emit in liquids but emit in solids because of the conjugation of lone electrons in solids [12]. It was speculated that the fluorescence enhancement and redshift of the series of fluorenone derivatives resulted from the formation of dimer/excimer [13], according to the con-



Scheme 1. Molecular structure of DPFO.

centration dependence on the fluorescence spectra and the crystal structures. However, theoretical calculations [14] suggest that the redshifted fluorescence should be the monomer emission, and the two fluorescence peaks seem to correspond to S_3 and S_1 emissions, respectively.

The reported both emission enhancement and large redshift of fluorenone derivatives in solids seem very fascinating but also somewhat self-contradictory. Typically, a redshift means that molecular structures containing several aromatic rings which can rotate along single bonds to adjust conjugation (like in Scheme 1) are more conjugated, and more planar. However, many molecules with more planar structures (compared to other less conjugated conformations of themselves) tend to stack better in solids and are easier to have ACQ instead of the AIE effect. Herein, to investigate this anti-intuitive and perplexing reported phenomenon, 2,7-diphenylfluorenone (DPFO) and 2,7-diphenyl-fluorene (DPF) are studied in detail with experiments and theory.

II. EXPERIMENTS

A. Synthesis

The 2,7-diphenylfluorenone (DPFO) were synthesized via a one-step Suzuki coupling reaction with 2,7-dibromo-9H-fluorene-9-one and phenylboronic acid. The synthesis details are consistent with Ref.[11], but the difference lies in the later separation. We used the dichloromethane (DCM)-petroleum ether (PE) (4:6, V/V) for secondary column chromatography. ^1H NMR (CDCl_3 , 400 MHz), δ/ppm : 7.94 (d, 2H), 7.75 (dd, 2H), 7.67–7.59 (m, 6H), 7.52–7.44 (m, 4H), 7.43–7.35 (m, 2H). FTMS-EI: calculated 332.1, found 332.1.

The 2,7-diphenylfluorene (DPF) were also synthesized via a one-step Suzuki coupling reaction with 2,7-dibromofluorene and phenylboronic acid, and purified by flash column chromatography over silica gel eluting with PE/DCM (10:1, V/V). ^1H NMR (CDCl_3 , 400 MHz), δ/ppm : 7.87 (d, 2H), 7.8 (s, 2H), 7.66 (m, 6H),

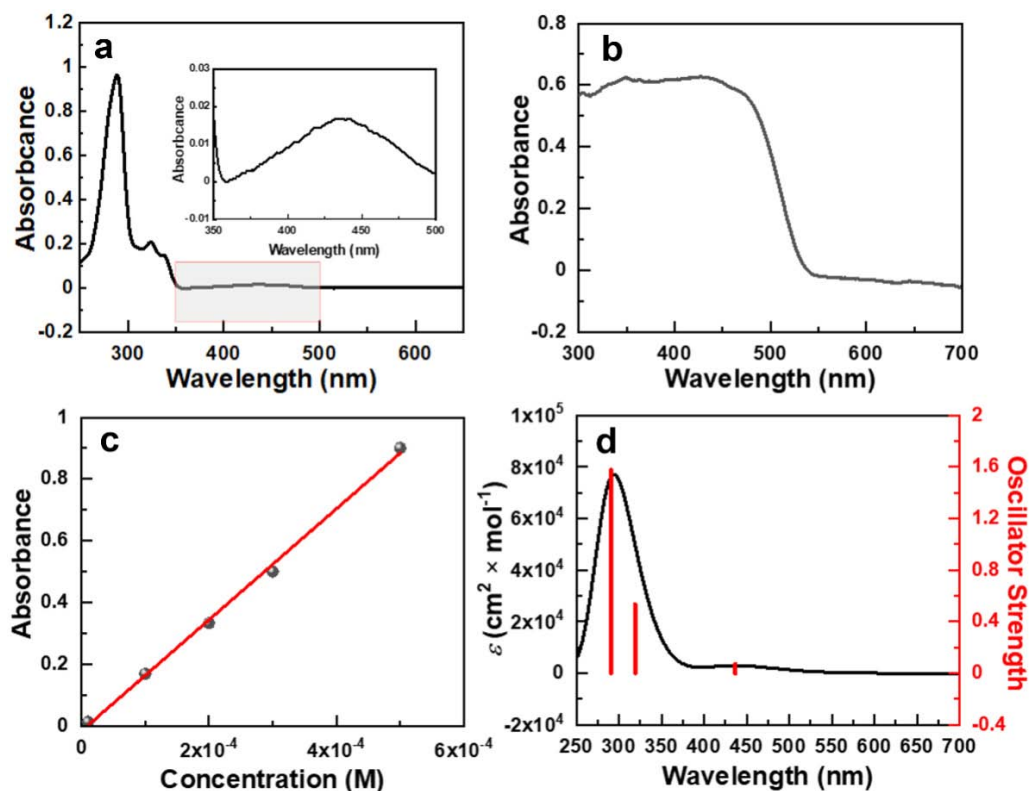


FIG. 1 (a) UV-visible absorption spectra of the DCM solutions (10 $\mu\text{mol/L}$) of DPFO, the insert is a partial enlargement of the spectrum. (b) UV-visible absorption spectra of DPFO solid. (c) The value of absorbance at 437 nm versus the concentration of the DCM solution of DPFO. DPFO are used as synthesized. (d) Calculated absorption spectrum of DPFO at the PBE0 levels, the red line indicates the three peaks where the oscillator strength is not zero.

7.47 (t, 4H), 7.36 (t, 2H), 4.03 (s, 2H). MALDI: calculated 318.1, found 318.1.

B. Spectroscopic characterization

UV-visible absorption spectra were recorded with Shimadzu UV3600Plus UV-VIS-NIR spectrophotometer. Photoluminescence (PL) spectra were recorded using a F7000 fluorescence spectrometer. The fluorescence quantum yield (Φ) and fluorescence lifetime were measured using an Edinburgh FLS980, the former using integrating sphere attachments.

C. Computational methods

All of the calculations presented here were performed using the Gaussian 16 suite. Geometry optimizations of DPF were carried out using density functional theory (DFT) with the M06-2X functional employing the 6-311++G(d, p). Vertical excitation energies were calculated using time-dependent DFT (TDDFT) with PBE0 functional employing the def2tzvp basis set. All of the

calculations herein were performed using the polarizable continuum model with DCM.

III. RESULTS AND DISCUSSION

FIG. 1 (a) and (b) show UV-visible absorption spectra of as-synthesized DPFO in DCM ($\sim 10 \mu\text{mol/L}$) and solid state, respectively. The three apparent absorption peaks in the solution are respectively at 289, 324, and 337 nm. It is noteworthy that the absorption peak at 437 nm is observable, which was previously reported to be the absorption of DPFO dimer and invisible at this concentration [11]. The absorption peak at 437 nm can also be observed in tetrahydrofuran (THF) solutions of $\sim 20 \mu\text{mol/L}$ (FIG. S1 in Supplementary materials).

If the peak at 437 nm was due to the dimer absorption as previously suggested, according to the Lambert Beer law and the monomer/dimer equilibrium, the increase of absorbance should be nonlinear with the increase of concentration because the dimer concentration is proportional to the square of monomer's concentration. However, in the concentration gradient experi-

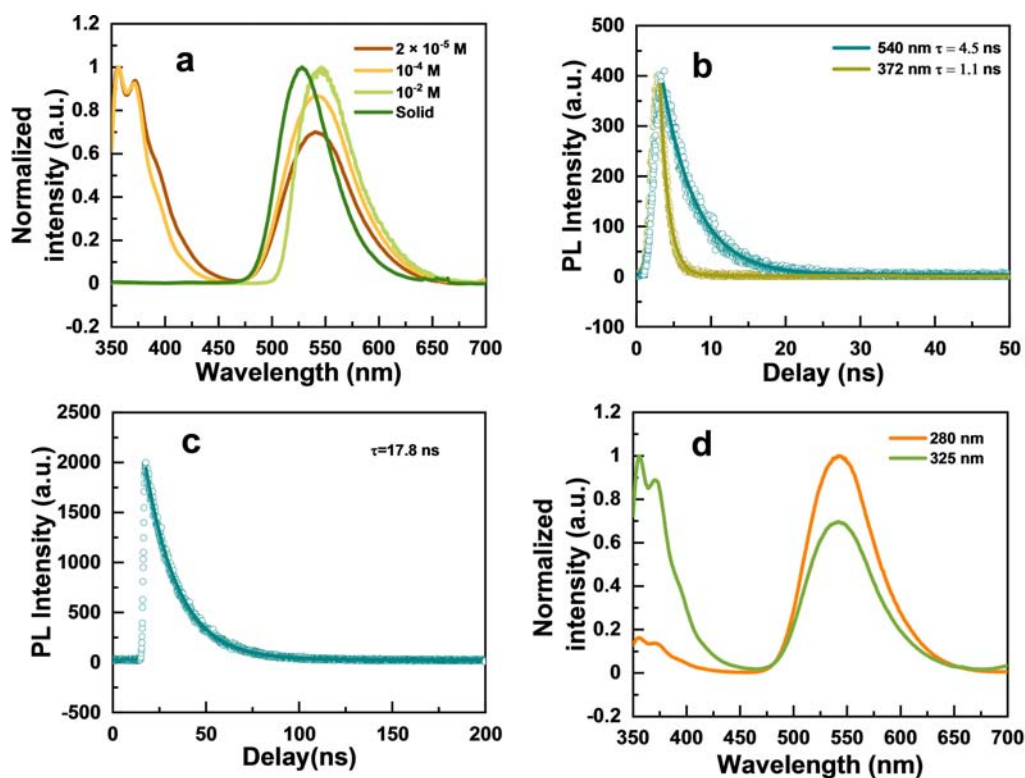


FIG. 2 (a) Normalized fluorescence spectra of DPFO in DCM at different concentrations and in solid with 325 nm excitation. (b) Fluorescence decays of DPFO in DCM (20 $\mu\text{mol/L}$) at different wavelengths with 320 nm excitation. (c) Fluorescence decay of DPFO in the solid state at 540 nm. (d) Normalized fluorescence spectra of DPFO in DCM (20 $\mu\text{mol/L}$) with 280 nm and 325 nm excitation respectively. DPFO are used as-synthesized.

ments, the concentration dependence of absorbance at 437 nm is linear (FIG. 1 (c)). In addition, the UV-Vis absorption spectrum of DPFO is calculated using TD-DFT. FIG. 1 (d) displays the calculated results. The absorption peaks are at 437, 319, and 288 nm, respectively, corresponding to the absorption of S_0-S_1 , S_0-S_3 , and S_0-S_5 of DPFO, consistent with experiments. These results suggest that the peak at 437 nm is probably the absorption of DPFO monomer instead of dimer.

FIG. 2(a) displays the fluorescence spectra of DPFO in DCM with different concentrations and in solid. The peak positions at 356, 372, and 540 nm are similar to those reported previously [11]. The relative intensities of the peaks show a concentration-dependent trend where the peaks at 356 and 372 nm become stronger in a more dilute solution compared to the peak at 540 nm, and the two peaks at 356 and 372 nm disappear in the concentrated solution (10^{-2} mol/L) and the solid. The trend is similar to that previously reported but the relative intensity of peak at 540 nm is higher than that reported in Ref.[11], which will be discussed in the fol-

lowing. The fluorescence lifetime at 372 nm in the dilute solution and at 528 nm in the solid state is 1.1 ns and 17.8 ns, respectively (FIG. 2(b, c)), consistent with Ref.[11]. The fluorescence lifetime at 540 nm in the dilute solution is 4.5 ns (FIG. 2(b)). The FL lifetime of peak at 528 nm in solid is more than 10 times longer than that of 372 nm in the dilute solution, which seems to be consistent with the reported huge AIE effect (enhancement of more than 10 times) accompanied with a large redshift (>150 nm).

However, when the molecule is excited to a higher energy level with 280 nm excitation (orange curve), the relative fluorescence intensity at 372 nm compared to that excited with a lower photonic energy 325 nm, as displayed in FIG. 2(d). The results are opposite to what would be expected if the peak at 372 nm was from monomer and the peak at 540 nm was from dimer as suggested previously. The longer FL wavelength of the dimer indicates that it probably has a longer absorption wavelength than the monomer [15]. Therefore, a longer excitation wavelength is expected to favor the

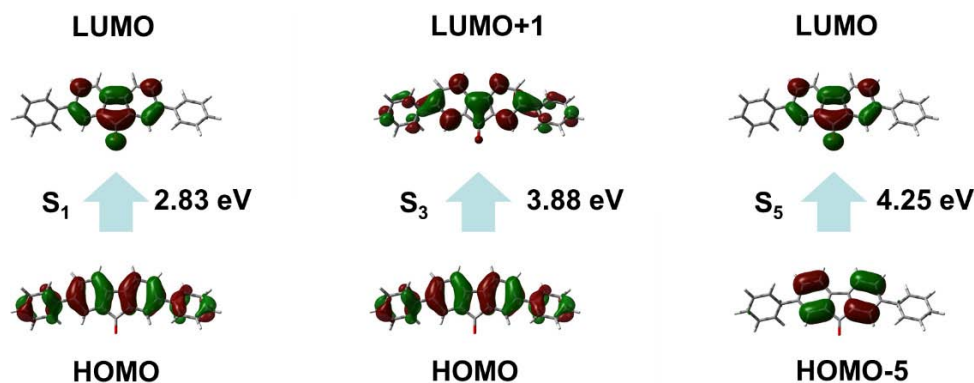


FIG. 3 The molecular orbitals involved in first three bright transitions (S_0-S_1 , S_0-S_3 , and S_0-S_5) of DPFO with the experimental absorption energies.

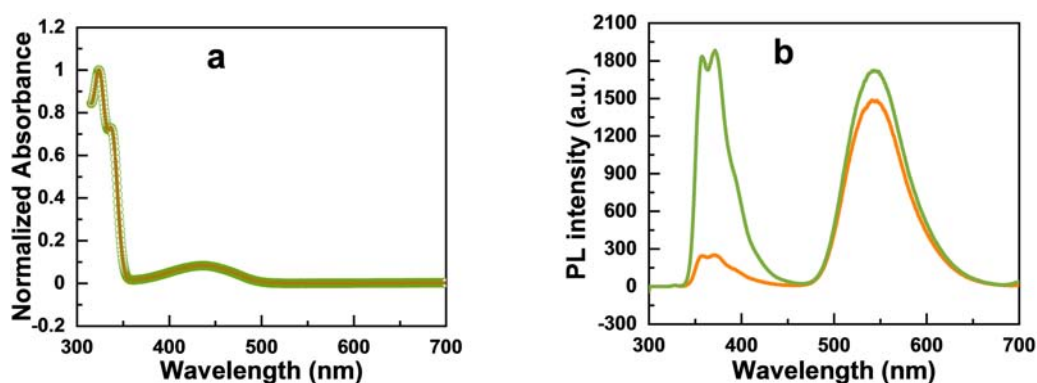


FIG. 4 (a) Normalized UV-visible absorption spectra, and (b) PL spectra ($\sim 20 \mu\text{mol/L}$) of DPFO in DCM solution which were synthesized at two different time. The green line is the first synthetic sample, the orange is the second.

dimer's FL rather than the opposite phenomenon that is observed in FIG. 2(d).

There are two possible mechanisms that can lead to the results in FIG. 2(d). One is that the two peaks are because of dual emissions, and the other is that the two peaks are from two different materials which have different structures and different FL intensities and wavelengths. Molecules can have dual emissions, either due to the evolution of excited state structure, like intramolecular proton transfer [16], or because the internal transformation of the excited state is very slow [17]. FIG. 3 shows the molecular orbitals involved in the three bright transitions and the corresponding energy gaps of DPFO. It is found that the transition of S_0-S_1 exhibits some charge transfer (CT) state behavior, and the energy gap between S_1 and S_3 is close to 1 eV. The results are similar to those reported by Ref.[14]. These results seem to imply that DPFO has dual emissions rather than the dimer emission. However, in repeated experiments with DPFO synthesized at different times, we discover that the relative intensities of the two fluorescence peaks ($\sim 372 \text{ nm}$ *vs.* $\sim 542 \text{ nm}$) at the same

concentration vary significantly, whereas the UV-Vis absorption spectra of the as-synthesized samples remain almost unchanged, as displayed in FIG. 4.

The results in FIG. 4 strongly suggest that the DPFO molecules synthesized at different time may contain different amounts of impurities which may significantly contribute to the observed fluorescence change (which also explains different peak 542/372 nm ratios observed in this work different from those in Ref.[11]). GC-MS characterizations indicate that the system contains some impurities (FIG. S3 in Supplementary materials). Therefore, we separate and collect both the impurities and pure DPFO with the aid of GC-MS. FIG. 5(a) displays the UV-Vis absorption spectrum of pure DPFO, which is almost identical to that shown in FIG. 1(a) for the as-synthesized sample containing impurities. There is a major peak at 288 nm, two shoulders at 324 and 337 nm, and a small peak at 437 nm. However, the pure DPFO only has a fluorescence peak of 542 nm (FIG. 5(b)) with a quantum yield about 4.5% in a dilute DCM solution with 325 nm excitation, instead of three (356, 372, and 542 nm) of the as-synthesized sample

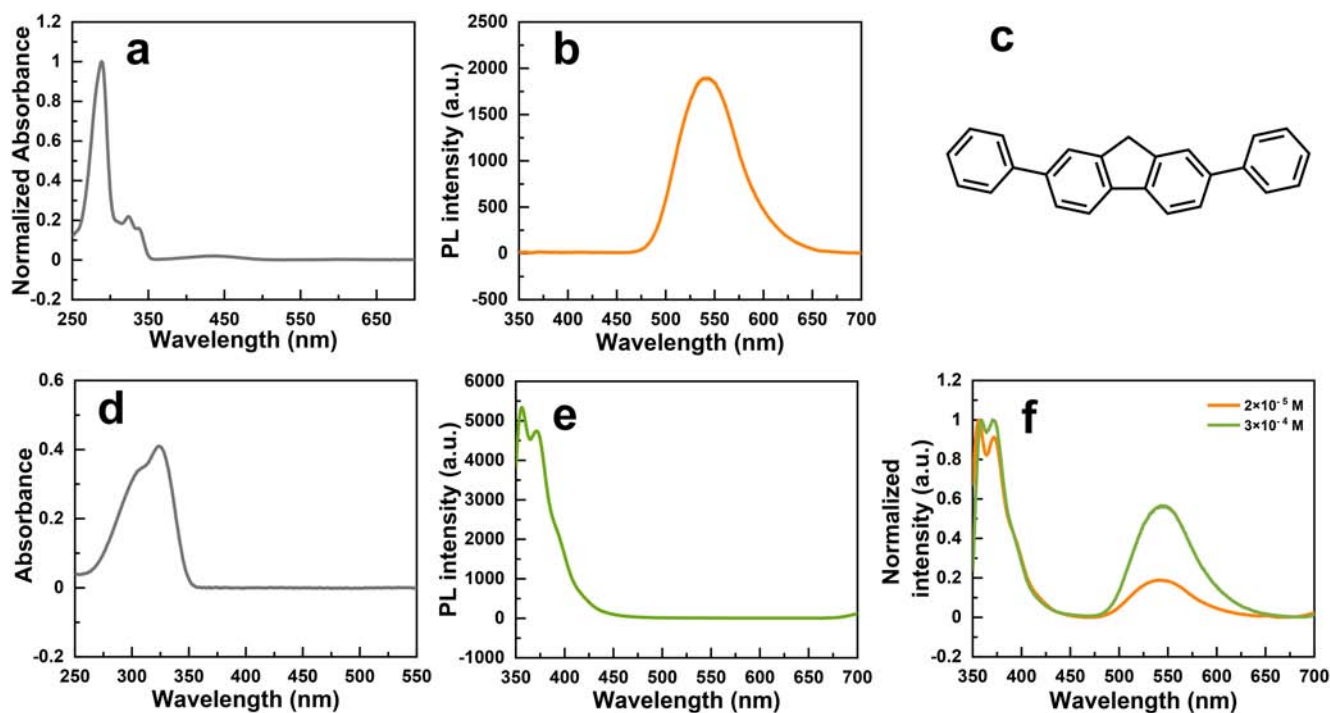


FIG. 5 (a) Normalized UV-visible absorption spectra of the DCM solutions (20 $\mu\text{mol/L}$) of DPFO. (b) Fluorescence spectra of DPFO in DCM (20 $\mu\text{mol/L}$) at 325 nm excitation. (c) Structure of DPF. (d) UV-visible absorption spectra of the DCM solutions of DPF. (e) Fluorescence spectra of DPF at 325 nm excitation. (f) Normalized fluorescence spectra of DPFO/DPF (100:1) in DCM at different concentrations.

(FIG. 2(a)). The luminescence spectrum of pure DPFO is similar in solvents with different polarities (FIG. S2 in Supplementary materials), implying that the three peaks are probably not because of solvent effects.

The impurities are analyzed. It turns out to be 2,7-diphenyl-fluorene (DPF), the structure is shown in FIG. 5(c). FIG. 5 (d) and (e) respectively display the UV-Vis absorption and fluorescence spectra of this impurity molecule. Its absorption peaks at 324 nm with a shoulder at 305 nm overlap with the absorption shoulder peaks of DPFO. Its fluorescence peaks appear at 356 nm and 372 nm. These two peaks are exactly the same as those in FIG. 2(d) for the as-synthesized DPFO solution which also contains DPF. In fact, significant differences in luminescence properties between fluorene and fluorenone have been recognized [18]. The amount of DPF is significantly smaller than DPFO in the as-synthesized sample, but the FL intensities of peaks at 372 nm (DPF) and 542 nm (DPFO) are similar. The results indicate that the FL quantum yield of DPF must be much bigger than DPFO, provided that the transition dipole moment of DPF is not significantly larger than DPFO. This is verified by experiments. DPF does have a quantum yield of about 90% in the

dilute solution with 320 nm excitation ($\sim 5 \mu\text{mol/L}$), about 20 times of DPFO. When 1% DPF is added into DPFO, the fluorescence spectra of this mixture (FIG. 5(f)) reproduce the change of relative peak intensities of the as-synthesized solution in FIG. 2(a) with 325 nm excitation. The observation can be well explained. Although the amount of DPF is only 1% of DPFO, both its absorption coefficient (or electronic transition dipole moment) at the excitation wavelength and FL quantum yield are larger than those of DPFO, leading to more prominent FL peaks at 356 and 372 nm (DPF) than at 542 nm (DPFO). With the increase of concentration, DPF and DPFO become closer, leading to faster electronic energy transfer from DPF to DPFO which effectively quenches DPF's FL at 356 and 372 nm but enhances DPFO's FL at 542 nm. This results in a relatively bigger peak at 542 nm in a more concentrated solution.

When the concentration is sufficiently high, *e.g.* 0.01 mol/L or bulk solid, DPF and DPFO are so close to each other that the energy transfer from DPF to DPFO becomes very fast and can effectively remove most of the electronic excitation from DPF, resulting

in the disappearance of peaks at 356 and 372 nm as shown in FIG. 2(a).

Therefore, the huge AIE effect associated with a large FL redshift of about 150 nm from \sim 380 nm to 530 nm of as-synthesized DPFO samples is not the inherent property of DPFO, but rather caused by the impurity DPF. For pure DPFO, its FL quantum yield is about 4.5% in a dilute DCM solution with a FL wavelength at 542 nm. In solid, its FL quantum yield is about 20% with a FL wavelength at 528 nm. It does have a FL enhancement in the solid state, but the enhancement factor is only about 4–5 times, which is consistent to the FL lifetime measurements (4.5 ns in dilute solution *vs.* 17.8 ns in solid). As expected and similar to traditional AIE molecules like TPE, the FL of DPFO wavelength in solid is slightly shorter than that in the dilute solutions, because the solid molecular environment imposes spatial constraints on DPFO which leads to a less conjugated molecular structure.

IV. CONCLUSION

In summary, the unusual AIE effect associated with a large FL redshift of as-synthesized DPFO samples is thoroughly investigated. It is found that the pure DPFO molecule does have an intense FL in solid, about 4–5 times larger than in its dilute solutions, but with a blueshifted rather than redshifted FL wavelength in solid. The enormous FL enhancement and redshifted FL wavelength of the as-synthesized DPFO solid are because of the presence of impurity DPF. DPF has shorter FL wavelengths and its FL is much stronger than that of DPFO. In the dilute solution of DPFO with DPF, the main fluorescence peaks come from DPF, even though the DPF content (\sim 1%) is very low. The electronic energy of DPF can transfer to DPFO because the electronic absorption peaks of DPF overlaps with DPFO. The closer the distance between DPF and the surrounding molecules, the faster the energy transfer, resulting in fluorescence quenching of DPF (356 and 372 nm). Therefore, at high concentrations or in solids, only peaks at about 542 or 528 nm show up and peaks at 356 and 372 nm disappear. This work explains the controversy over DPFO's luminescence.

Supplementary materials: The absorption and emission spectra in different solvents, GC-MS spectra, and ^1H NMR spectra of DPFO or DPF are provided.

V. ACKNOWLEDGMENTS

This work was supported by the National Natural Science Foundation of China (No.21627805, No.21673004, No.21804004, and No.21821004) and Ministry of Science and Technology of China (No.2017YFA0204702).

- [1] J. Mei, N. L. Leung, R. T. Kwok, J. W. Lam, and B. Z. Tang, *Chem. Rev.* **115**, 11718 (2015).
- [2] J. Luo, Z. Xie, J. W. Y. Lam, L. Cheng, B. Z. Tang, H. Chen, C. Qiu, H. S. Kwok, X. Zhan, Y. Liu, and D. Zhu, *Chem. Commun.* **18**, 1740 (2001).
- [3] G. C. Schmidt, *Ann. Phys.* **294**, 103 (1896).
- [4] Y. Hong, H. Xiong, and J. W. Lam, M. Häussler, J. Liu, Y. Yu, Y. Zhong, H. H. Sung, I. D. Williams, K. S. Wong, and B. Z. Tang, *Chemistry* **16**, 1232 (2010).
- [5] F. Hu, S. Xu, and B. Liu, *Adv. Mater.* **30**, e1801350 (2018).
- [6] J. Guan, R. Wei, A. Prlj, J. Peng, K. H. Lin, J. Liu, H. Han, C. Corminboeuf, D. Zhao, Z. Yu, and J. Zheng, *Angew. Chem. Int. Ed.* **59**, 14903 (2020).
- [7] F. Meinardi, M. Cerminara, A. Sassella, R. Bonifacio, and R. Tubino, *Phys. Rev. Lett.* **91**, 247401 (2003).
- [8] J. Xue, Q. Liang, R. Wang, J. Hou, W. Li, Q. Peng, Z. Shuai, and J. Qiao, *Adv. Mater.* **31**, e1808242 (2019).
- [9] C. M. Mauck, P. E. Hartnett, E. A. Margulies, L. Ma, C. E. Miller, G. C. Schatz, T. J. Marks, and M. R. Wasielewski, *J. Am. Chem. Soc.* **138**, 11749 (2016).
- [10] J. Guan, C. Shen, J. Peng, and J. Zheng, *J. Phys. Chem. Lett.* **12**, 4218 (2021).
- [11] M. S. Yuan, D. E. Wang, P. Xue, W. Wang, J. C. Wang, Q. Tu, Z. Liu, Y. Liu, Y. Zhang, and J. Wang, *Chem. Mater.* **26**, 2467 (2014).
- [12] R. B. Wang, W. Z. Yuan, and X. Y. Zhu, *Chin. J. Polym. Sci.* **33**, 680 (2015).
- [13] F. Xu, H. Wang, X. Du, W. Wang, D. E. Wang, S. Chen, X. Han, N. Li, M. S. Yuan, and J. Wang, *Dyes Pigm.* **129**, 121 (2016).
- [14] D. Presti, L. Wilbraham, C. Targa, F. Labat, A. Pedone, M. C. Menziani, I. Ciofini, and C. Adamo, *J. Phys. Chem. C* **121**, 5747 (2017).
- [15] M. W. Frangoise, *Chem. Rev.* **93**, 587 (1993).
- [16] H. W. Tseng, J. Y. Shen, T. Y. Kuo, T. S. Tu, Y. A. Chen, A. P. Demchenko, and P. T. Chou, *Chem. Sci.* **7**, 655 (2016).
- [17] Q. J. Meisner, A. H. Younes, Z. Yuan, K. Sreenath, J. J. M. Hurley, and L. Zhu, *J. Phys. Chem. A* **122**, 9209 (2018).
- [18] K. L. Jeong-I, K. Gerrit, and D. M. Robert, *Chem. Mater.* **11**, 1083 (1999).